Fiber-to-Waveguide Alignment Assisted by a Transparent Integrated Light Monitor

Marco Carminati, *Member, IEEE*, Stefano Grillanda, Pietro Ciccarella, Giorgio Ferrari, *Member, IEEE*, Michael J. Strain, Marco Sampietro, Andrea Melloni, *Member, IEEE*, and Francesco Morichetti, *Member, IEEE*

I. Introduction

SIMPLE, robust and accurate solutions for automatic alignment of optical fibers to photonic waveguides are fundamental for both testing and packaging of photonic integrated circuits [1]. In fact, the connection of photonic chips to one or more optical fibers still represents a challenge, with impact on the performance, cost, reliability and manufacturability of the photonic system [2]. Alignment techniques can be divided into passive and active, the latter requiring a light source and an optical detector. The optimum choice depends on the waveguide technology, size and cross-sectional shape [3]. Given a maximum tolerable level of coupling loss, the most relevant parameters setting the required spatial accuracy are the sizes of the fiber mode and of the waveguide mode, as well as the constraints imposed by mode size converters such as lenses, tapers or grating couplers. In general, passive techniques, simply relying on the mechanical slotting-in of the fiber into properly shaped structures such as V-grooves [4], are limited to an accuracy of ~1 μm, the state of the art being represented by the 0.5 μm repeatability achieved with microfabricated alignment features for 1.9 μm indium phosphide (InP) waveguides [5]. Efficient coupling (0.6 dB loss per facet) has been obtained for single mode fibers passively aligned to 5 μm buried sol-gel/SiON waveguides [6].

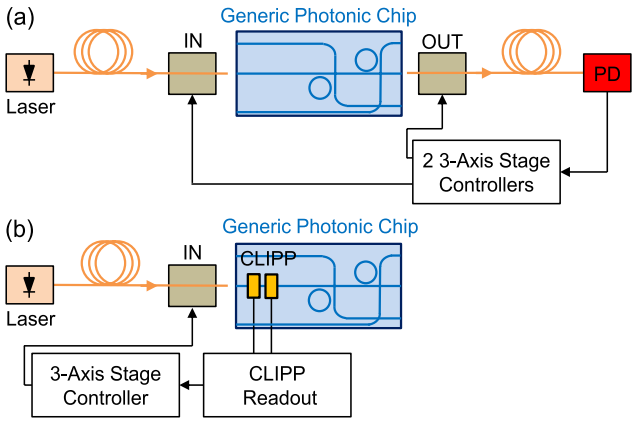

Fig. 1. (a) Conventional approach for the alignment to photonic chips, that requires an input fiber from the laser to the chip, and an output fiber that feeds an external photodetector. (b) The proposed approach, based on an integrated transparent light monitor (CLIPP), that requires only one fiber. The square boxes labeled with "IN" and "OUT" represent the positioning stages of the fibers.

Active techniques, instead, allow the attainment of an accuracy of ~100 nm, suitable for waveguides with sub-micron cross-sectional dimensions, such as in silicon (Si) photonics, yet at the price of a more time consuming process and, typically, of a more complex alignment setup. State of the art solutions exploit sophisticated packaging toolboxes for automated fiber pigtailing both on InP and silicon-on-insulator (SOI) platforms [7] and vertical coupling to monolithic photonic-CMOS wafers by means of grating couplers [8].

In the case of photonic devices lacking integrated photodetectors, the traditional alignment process, illustrated in Fig. 1a, requires the simultaneous alignment of two optical fibers [9]: one to couple the light from the laser source to the chip, the other to collect the output light and feed an external photodetector (PD) that closes the feedback loop tracking the light coupling process. This approach presents two main drawbacks: (i) two fiber interfaces must be aligned at the same time (from a control point of view, this is an ill-posed

Manuscript received September 1, 2014; revised November 10, 2014; accepted December 11, 2014. Date of publication December 18, 2014; date of current version February 11, 2015. This work was supported in part by the European Commission within the FP7-ICT Project through the Breaking the Barriers of Optical Integration and in part by the Fondazione Cariplo.

M. Carminati, S. Grillanda, P. Ciccarella, G. Ferrari, M. Sampietro, A. Melloni, and F. Morichetti are with the Dipartimento di Elettronica, Informazione e Bioingegneria, Politecnico di Milano, Milan 20133, Italy (e-mail: marco1.carminati@polimi.it; stefano.grillanda@polimi.it; pietro.ciccarella@polimi.it; giorgio.ferrari@polimi.it; marco.sampietro@polimi.it; andrea.melloni@polimi.it; francesco.morichetti@polimi.it).

M. J. Strain is with the Institute of Photonics, University of Strathclyde, Glasgow G1 1XQ, U.K. (e-mail: michael.strain@strath.ac.uk).

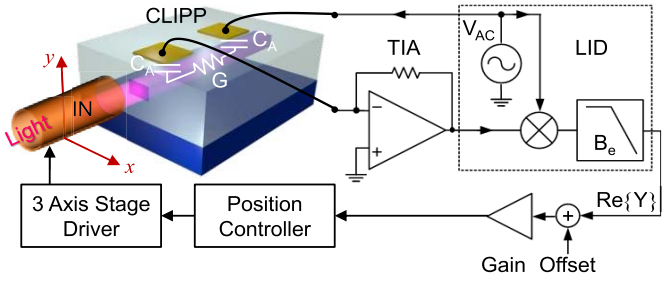

Fig. 2. Architecture of the system that performs the CLIPP readout operations, and uses the CLIPP feedback signal to drive the fiber-to-waveguide alignment position.

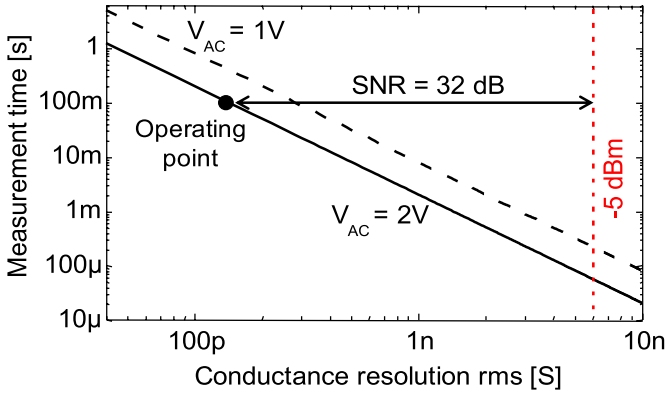

Fig. 3. Trade-off between the speed and resolution of the CLIPP for an applied voltage V_{AC} of 1 V (dashed line) and 2 V (solid line).

problem, since many degrees of freedom must be optimized with a single feedback signal); (ii) the light intensity coupled to the output fiber depends on the "health" status and topology of the circuit, and on the wavelength, so that information on the circuit performance is required to assess the effectiveness of the alignment.

This letter presents an original active technique that leverages an integrated, transparent, in-line light monitor [10] for single fiber alignment to a generic photonic chip, regardless of the complexity and operation point of the optical circuit (Fig. 1b). The presented technique applies both to edge and vertical coupling to optical waveguides. In Sec. II the design of the alignment loop is presented, including a description of the relevant blocks, starting from the embedded monitor. Sec. III shows the results of the spatial mapping of the edge coupling, while examples of manual and automatic alignment are reported in Sec. IV. Finally, Sec. V contains concluding comments on the impact and applicability of this technique.

II. System Design

A. Working Principle of the CLIPP Monitor

The proposed alignment approach is illustrated in Fig. 1b. The CLIPP [10] is composed of two metal electrodes that are placed on top of the cladding of the photonic waveguide near the chip input facet, and provides an electric feedback signal to steer the fiber positioning, and eliminates the need for an optical output. In this way both major drawbacks of the traditional double-fiber approach are circumvented.

The CLIPP working principle, which is explained in detail in [10], relies on the non-invasive measurement of the electric conductance of a semiconductor optical waveguide. The waveguide conductance changes with light intensity because of the free carriers that are generated by surface state absorption mechanisms [11], that are associated with intrinsic mid-gap energy states existing at the core/cladding interface. In order to perform the measurement of the photogenerated carriers without any light perturbation, the waveguide is probed through a remote capacitive access. The access capacitance C_A is given by the insulating upper cladding between the waveguide core and the metal electrodes of the CLIPP, which are sufficiently spaced from the core to avoid additional optical loss (Fig. 2). The CLIPP electrodes can be fabricated with any CMOS-compatible metal technology [12].

B. Experimental Setup and Feedback Architecture

The scheme of the proposed CLIPP-assisted closed-loop active alignment architecture is shown in Fig. 2. An external sinusoidal voltage V_{AC} is applied to the CLIPP electrodes making the photogenerated carriers oscillate with no significant effect on light propagation [10]. A transimpedance amplifier (TIA) converts the CLIPP alternating current into an output voltage, which is then demodulated and low-pass filtered by a phase-sensitive lock-in detector (LID). The real component $G = \mathrm{Re}\{Y\}$ of the measured admittance Y is a function of the optical power P travelling in the waveguide [10]. Thanks to this relation, the signal provided by the LID needs only to be scaled in order to match the input voltage range of the fiber positioning controller. It is worth noticing that all the electronic readout circuitry can be integrated in a single CMOS chip, providing extreme setup miniaturization, potential for monolithic CMOS integration, multichannel parallelization and performance improvement [12].

The CLIPP electrodes are placed in proximity of the input facet, in order to make the alignment procedure independent of the circuit integrated on the photonic chip. Therefore, the optical power coupled into the waveguide is about the same as the power at the CLIPP input. For the experiments reported here, the operating wavelength is 1550 nm, and a channel Si waveguide (220 nm thick and 1 μm wide), fabricated on a 2 μm-thick bottom oxide is utilized. The 200 μm long electrodes of the CLIPP are separated by 100 μm, and are placed on top of the 1 μm thick SiO_2 top cladding, so that they do not induce any additional loss or appreciable perturbation to the waveguide [10]. This geometry has been designed for an optimal operating frequency $f_{AC} = 2$ MHz that enables the bypassing of the vertical access capacitances C_A to directly probe G. Details on the scalability of the CLIPP design can be found in [12].

The response time of the alignment technique is set by the bandwidth B_e of the LID low-pass filter, which in this setup represents the dominating time constant of the feedback loop. The bandwidth B_e and the applied voltage V_{AC} can be adjusted to optimize the trade-off between the CLIPP time response and the signal to noise ratio (SNR): a larger B_e provides a faster response, yet at the price of higher noise that increases with the square root of B_e [12]. As illustrated in Fig. 3,

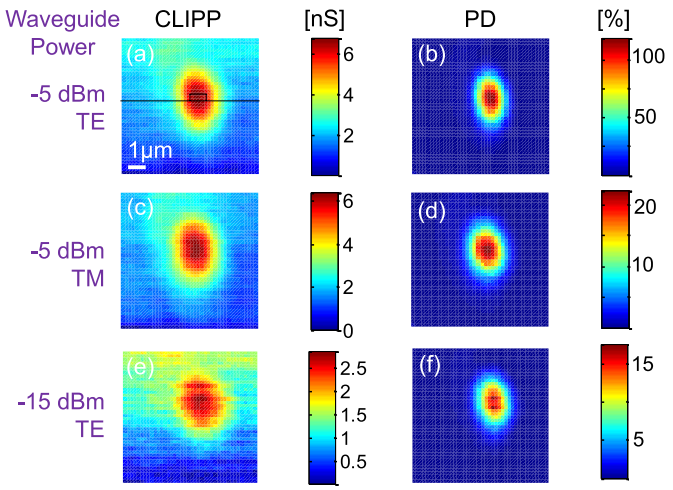

Fig. 4. Mapping of the spatial coupling between the lensed optical fiber and the waveguide with the CLIPP ($V_{AC} = 2$ V, $f_{AC} = 2$ MHz, $Be = 10$ Hz) and the PD for different power coupled into the waveguide and both polarizations.

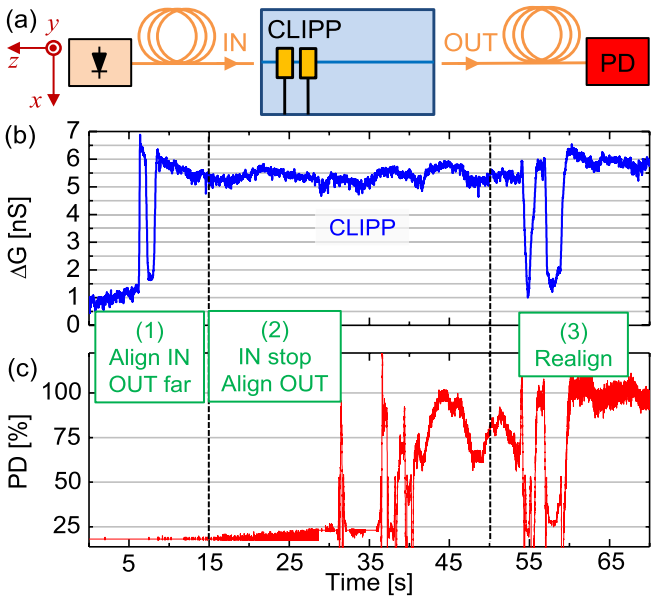

Fig. 5. (a) Setup to measure both the CLIPP (b) and the PD (c) signals for manual alignment of the (1) input fiber, (2) output fiber and (3) input fiber.

with $B_e = 10$ Hz (average time ~100 ms) the measured detection resolution improves with V_{AC}, changing from ~240 pS rms for $V_{AC} = 1$ V (dashed line) to ~140 pS rms for $V_{AC} = 2$ V (solid line). At the optical waveguide power of −5 dBm used for the alignment procedure (see Sec. IV), corresponding to a waveguide conductance variation $\Delta G = 6$ nS (red dashed line), a SNR of about 32 dB is achieved. The alignment system described in the following operates with $B_e = 10$ Hz, $V_{AC} = 2$ V (circle in Fig. 3) and time steps of 250 ms, accounting also for mechanical damping of the fiber tip.

III. Spatial Mapping of the Edge Coupling

A bare Si waveguide is used to compare the electrical signal provided by the CLIPP with the optical signal detected by a standard PD coupled to an output fiber. The position of the input fiber is systematically scanned in the xy plane parallel to the chip facet (see Fig. 2), exploring an area of 8 μm by 8 μm with steps of 200 nm (each step corresponds to a pixel of the maps reported in Fig. 4), and simultaneously recording both the CLIPP and PD signals in every point. Scans are repeated for different power levels and for both TE and TM polarizations. The profile maps show that the spatial extension of the fiber-to-waveguide coupling is about 2 μm, which is consistent with the diameter of the lensed fiber spot (that is about 1.7 μm at 1/e field amplitude). The wider vertical profile of the power coupling is related to the stronger free-space divergence of the modes on the vertical plane, which is due to the strongly asymmetric shape of the modes (much larger than higher in the considered waveguide). For an optical power of −5 dBm coupled into the waveguide (−10 dB coupling efficiency), the matching between the CLIPP (Fig. 4a) and PD (normalized in maximum power, Fig. 4b) signals is excellent, demonstrating the effectiveness of the CLIPP-assisted approach. Interestingly, the maps show that for the considered waveguide there is no significant difference in the CLIPP signals between the TE (Fig. 4a) and TM (Fig. 4c) polarizations. Therefore, CLIPP-assisted alignment can be achieved regardless of the polarization state of the input light.

As shown in Fig. 4e, when reducing the waveguide power down to −15 dBm, the Gaussian peak of the CLIPP signal remains clearly detectable. The operation of the CLIPP at this power level was demonstrated in a previous work [10], where we showed a sensitivity of down to −30 dBm, corresponding to a power density in the waveguide of about 1 kW/cm^2.

IV. Alignment Assessment

A. Manual Alignment

The validation of the CLIPP-assisted fiber alignment was initially carried out by means of a manually-operated procedure. As illustrated in Fig. 5a, the output fiber and the external PD are used here only for crosschecking the achievement of optimum alignment of the input fiber. To this end, the CLIPP and PD signals are synchronously recorded. As a starting condition, both fibers are manually positioned along the z direction in order to be close to the chip facets under microscope visualization, while they are far from the waveguide in the xy plane. Then, the input fiber only is moved (along xy directions) to maximize the signal measured by the CLIPP. When the input fiber is well aligned to the waveguide, only the CLIPP signal is maximum (Fig. 5b1), while the optical intensity collected at the output by the photodetector is still low (Fig. 5c1), since the output fiber is misaligned with respect to the photonic waveguide. The PD signal increases when the output fiber position is also changed, and is maximal when the optimum output alignment is reached. It is worth noticing that during this interval (Fig. 5b2), i.e. when the position of the output fiber only is changed, the CLIPP signal does not vary, since it is not affected by what happens downstream. This makes the presented approach useful for the

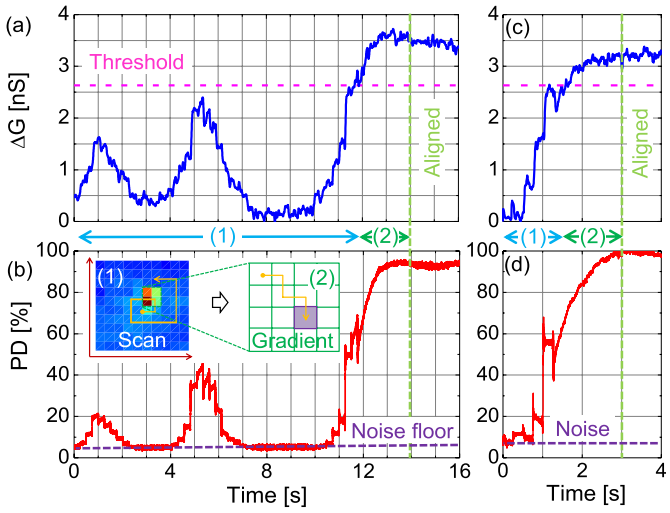

Fig. 6. Closed-loop automated alignment assessment by recording the CLIPP and the normalized PD signals, starting from a 17 μm distance (a-b) and 4 μm (c-d), leading to a total alignment time of 14 s and 3 s respectively. The two-step algorithm starts with a distance-dependent spiral scan and, after 2.6 nS threshold passing, terminates with a max. gradient fine optimization.

alignment of generic and arbitrarily complex photonic circuits, regardless of their operating point and status.

In order to prove the agreement between the signals provided by the two detectors, once the output fiber is aligned, the input fiber is moved away and realigned again. As shown in Fig. 5b3, the CLIPP provides the same information as the external PD, without requiring alignment of the output fiber.

B. Automatic Alignment

Here we present the assessment of the automatic CLIPP-assisted fiber alignment with a custom computer-based closed-loop algorithm. Nevertheless, since the CLIPP detector can be employed as a conventional power monitor, any kind of alignment algorithm can be used. As shown in Fig. 6, the automatic algorithm consists of two phases. During the first phase a systematic spiral scan exploring the whole *xy* plane (range 20 μm by 20 μm) with coarse steps of 1 μm, starting from the central position, is performed, phase (1) in Fig. 6. When a properly-set threshold on the CLIPP signal is exceeded (here a robust 60% of the peak conductance), the scan is stopped and a second phase takes place. A hill climbing algorithm is run, exploring the power values in the neighboring pixels (step size 40 nm), and following the max. gradient direction until the peak is reached, phase (2) in Fig. 6.

Two alignment examples are reported in Fig. 6, differing from the initial distance from the max. coupling point, which determines the duration of the initial scan. For a start distance of $\sim$17 μm Fig. 6a-b, the scan time is 12 s, while for a smaller distance ($\sim$3 μm), it is reduced to only 1.2 s Fig. 6c-d. Once the threshold is exceeded, the max. gradient takes 2 s to reach optimal alignment in both cases. A total alignment time of a few seconds (from 3 s to 14 s) confirms the suitability of the CLIPP for automatic setups; if necessary, faster alignment could be achieved with improved control laws [13]. Further, due to the high SNR of the CLIPP detector (see Fig. 3 and Fig. 4), no degradation of the alignment accuracy ($\pm$0.2 dB) is observed compared to the conventional alignment approach (PD) performed on the same optical setup.

V. Conclusion

A novel fiber-to-waveguide alignment solution, exploiting a transparent integrated light monitor, has been demonstrated to enable the optical coupling of a fiber to a photonic chip. Accurate (40 nm) and fast (few seconds) automated fiber alignment was shown on a silicon photonic chip, but the CLIPP detector is compatible with any semiconductor waveguide technology, such as for instance InP.

The proposed technique is compatible with both edge and vertical coupling, and is particularly promising for packaging purposes since, once optimum alignment is achieved, the connection to the CLIPP electrodes can be removed. Alternatively, if continuous tracking and continuous closed-loop optimization of the maximum fiber-to-chip coupling is desired, the electrodes can be permanently connected to the readout electronics by means of bonding wires [12].

Furthermore, the presented approach is also promising for wafer-level testing. In this application, not only can CLIPP monitors can be used to assist the fiber alignment with vertical grating couplers, but they can also be exploited as integrated probes to inspect the "health" status of photonic circuits at a large number of hot spots before chip dicing.

References

[1] T. Baehr-Jones, T. Pinguet, P. L. Guo-Qiang, S. Danziger, D. Prather, and M. Hochberg, "Myths and rumours of silicon photonics," *Nature Photon.*, vol. 6, pp. 206–208, Mar. 2012.

[2] C. Kopp *et al.*, "Silicon photonic circuits: On-CMOS integration, fiber optical coupling, and packaging," *IEEE J. Sel. Topics Quantum Electron.*, vol. 17, no. 3, pp. 498–509, May/Jun. 2011.

[3] G. Böttger, H. Schröder, and R. Jordan, "Active or passive fiber-chip-alignment: Approaches to efficient solutions," *Proc. SPIE*, vol. 8630, pp. 863006-1–863006-17, Feb. 2013.

[4] R. Hauffe, U. Siebel, K. Petermann, R. Moosburger, J. Kropp, and F. Arndt, "Methods for passive fiber chip coupling of integrated optical devices," *IEEE Trans. Adv. Packag.*, vol. 24, no. 4, pp. 450–455, Nov. 2001.

[5] J. F. C. van Gurp, M. Tichem, U. Staufer, and J. Zhao, "Passive photonic alignment with submicrometer repeatability and accuracy," *IEEE Trans. Compon. Packag. Technol.*, vol. 3, no. 11, pp. 1971–1979, Nov. 2013.

[6] A. K. Chu and S. F. Hong, "Buried sol-gel/SiON waveguide structure for passive alignment to single-mode fiber on Si substrate," *IEEE Photon. Technol. Lett.*, vol. 19, no. 1, pp. 45–47, Jan. 1, 2007.

[7] L. Zimmermann, G. B. Preve, T. Tekin, T. Rosin, and K. Landles, "Packaging and assembly for integrated photonics—A review of the ePIXpack photonics packaging platform," *IEEE J. Sel. Topics Quantum Electron.*, vol. 17, no. 3, pp. 645–651, May/Jun. 2011.

[8] A. Mekis *et al.*, "A grating-coupler-enabled CMOS photonics platform," *IEEE J. Sel. Topics Quantum Electron.*, vol. 17, no. 3, pp. 597–608, May/Jun. 2011.

[9] J. H. Song, J. Zhang, H. Zhang, C. Li, and G. Q. Lo, "Si-photonics based passive device packaging and module performance," *Opt. Exp.*, vol. 19, no. 19, pp. 18020–18028, 2011.

[10] F. Morichetti *et al.*, "Non-invasive on-chip light observation by contactless waveguide conductivity monitoring," *IEEE J. Sel. Topics Quantum Electron.*, vol. 20, no. 4, pp. 292–301, Jul./Aug. 2014.

[11] M. Borselli, T. Johnson, and O. Painter, "Beyond the Rayleigh scattering limit in high-Q silicon microdisks: Theory and experiment," *Opt. Exp.*, vol. 13, no. 5, pp. 1515–1530, 2005.

[12] S. Grillanda *et al.*, "Non-invasive monitoring and control in silicon photonics using CMOS integrated electronics," *Optica*, vol. 1, no. 3, pp. 129–136, 2014.

[13] Y. Zheng and J.-A. Duan, "Alignment algorithms for planar optical waveguides," *Opt. Eng.*, vol. 51, no. 10, p. 103401, 2012.